JOURNAL OF MAGNETIC RESONANCE **125,** 372–375 (1997)
ARTICLE NO. MN971123

Suppression of Convection Artifacts in Stimulated-Echo Diffusion Experiments. Double-Stimulated-Echo Experiments

ALEXEJ JERSCHOW AND NORBERT MÜLLER*

Institut für Chemie, Johannes Kepler University Linz, Altenbergerstraße 69, A-4040 Linz, Austria

Received December 9, 1996

Convection within the sample is a serious problem affecting diffusion measurements, in particular at elevated temperatures. Convection currents are caused by small temperature gradients in the sample and cause additional signal decay that can be mistaken for faster diffusion. Recently, sophisticated multidimensional diffusion-ordered techniques such as DOSY (*1, 2*), DOSY–NOESY (*3*), COSY–DOSY (*4*), PFG–TOCSY (*5*), and DO–TOCSY (*6*) have been introduced into high-resolution NMR. In order to increase resolution and robustness of these methods in the diffusion dimension, convection artifacts must be suppressed. Some improvement can be made, e.g., by sample rotation (*7*), special sample cells, or by use of transverse gradients, but in general it is difficult to eliminate this problem entirely. We have also experienced severe interference by convection at temperatures close to ambient, probably due to pulsatile heating.

Here we present a pulse sequence which suppresses effects of convection in stimulated-echo (STE) diffusion experiments to first order provided that the convection current has a constant laminar flow profile during the diffusion interval of the pulse sequence. This condition is fulfilled in many systems of practical relevance. However, turbulent convection cannot be compensated for by this method.

In the usual NMR probe setup for superconducting vertical magnets, convection is mainly caused by a temperature gradient along the z axis, which is also the main axis of the cylindrical sample and the static field axis. Within the active volume of the sample, convection transports equal amounts of liquid in opposite directions in the inner and outer flow layers. We assume as a prerequisite that the convection velocity is constant during the diffusion delay in the experiment.

For the following discussion, we factor the amplitude dependence of the signals in STE-type experiments into a gradient-dependent term f_G and a relaxation-dependent term f_R. The gradient-dependent signal attenuation $f_G(t)$ in any gradient-echo sequence can be derived from the Bloch–Torrey equations (*8*) as

$$f_G(t) = \underbrace{\exp\left[-D\gamma^2\int_0^t\left(\int_0^{t'}\mathbf{g}^*(t'')dt''\right)^2dt'\right]}_{A(t)} \times \underbrace{\exp\left[i\gamma\mathbf{v}\int_0^t\left(\int_0^{t'}\mathbf{g}^*(t'')dt''\right)dt'\right]}_{B(t)}, \quad [1]$$

where D is the diffusion coefficient, $\mathbf{v}$ is the flow velocity, and $\mathbf{g}^*(t)$ is the effective gradient which is defined (in homonuclear spin systems) as $\mathbf{g}^*(t) = p(t)\cdot\mathbf{g}(t)$, where $p(t)$ is the coherence order and $\mathbf{g}(t)$ is the B_0-field gradient at time t. $A(t)$ represents the diffusion-dependent *amplitude* attenuation factor (which we would like to determine) while $B(t)$ is the interfering flow-velocity-dependent *phase* factor. It is fairly straightforward to separate these two effects when the flow is unidirectional. However, in diffusion measurements, convection just causes the signal amplitude to decrease due to the superposition of different velocities in the sample. Since equal numbers of molecules move upward and downward, all imaginary parts cancel over the sample volume. Hence, the average of $B(t)$ essentially becomes a damping factor like $A(t)$ in the case of a gradient-echo experiment.

The phase factor $B(t)$ can be made velocity independent by use of gradient sequences whose first moment is zero (*8*), i.e.,

$$\int_0^t\mathbf{g}^*(t')t'dt' = 0. \quad [2]$$

Such velocity-compensated gradients can conveniently be applied in simple gradient-echo experiments as shown in Fig. 1a. By nulling higher moments, one can eliminate second-order effects, i.e., flow acceleration.

We extend this approach to stimulated-echo experiments as, e.g., that in Fig. 1b (*9*). A double-stimulated-echo (DSTE) experiment as presented in Fig. 1c refocuses all

* To whom correspondence should be addressed.

1090-7807/97 $25.00

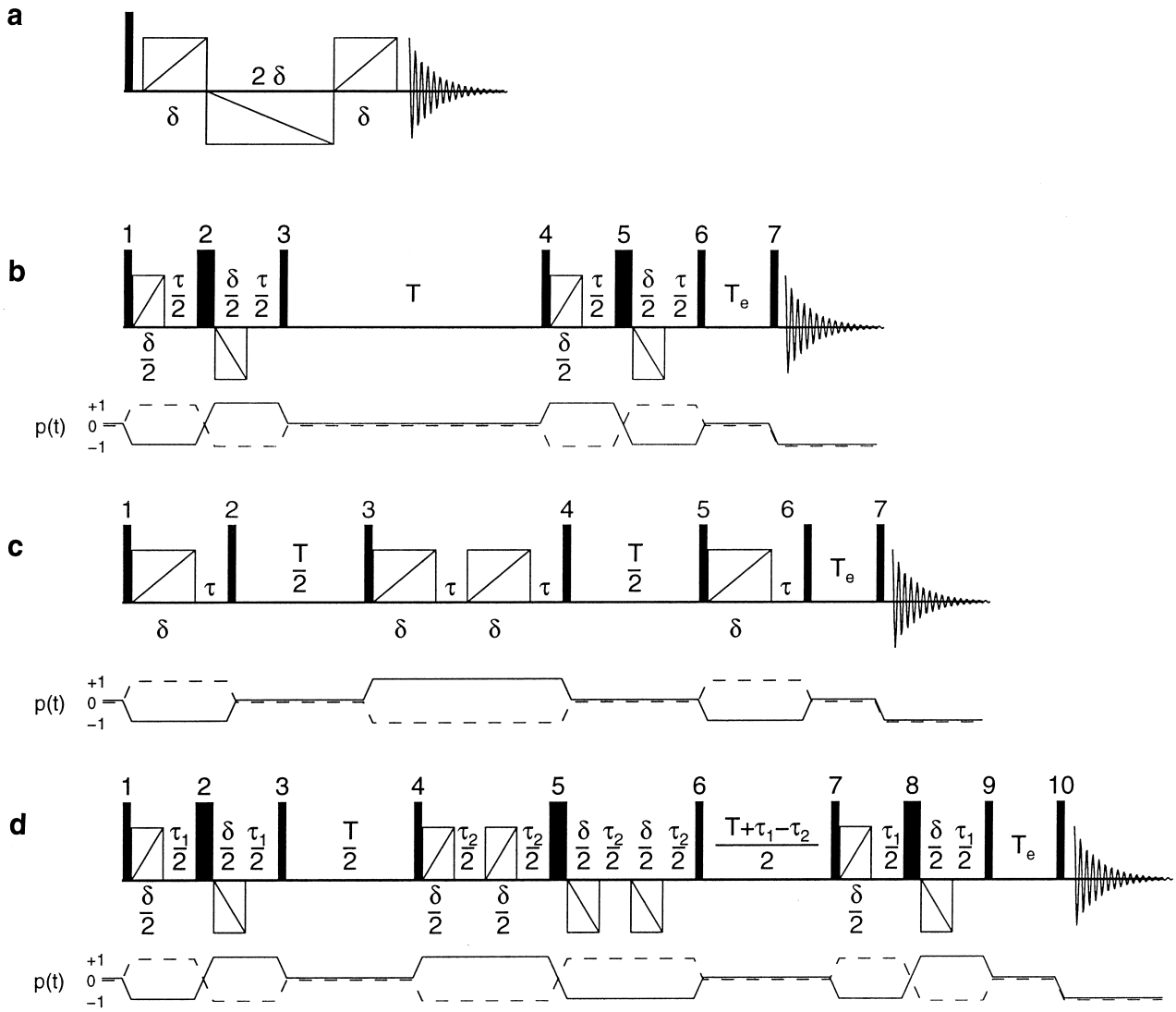

FIG. 1. (a) Simple gradient spin-echo pulse sequence with a zero first moment of the gradients. (b) Stimulated-echo pulse sequence with bipolar gradient pulses. The phase cycle is $\phi(1) = x, x, y, y, -x, -x, -y, -y$; $\phi(2) = y, -x, -x, -y, -y, x, x, y$; $\phi(3) = \phi(5) = x$; $\phi(4) = -x, -x, -y, -y$; $\phi(7) = -y, -y, x, x$; $\phi(6) = -x$; $\phi(\text{receiver}) = 2(x, -x), 2(-x, x)$. (c) Double-stimulated-echo experiment compensated for flow. The phase cycle is $\phi(1) = x, y, -x, -y$; $\phi(2) = \phi(5) = \phi(6) = \phi(7) = x$; $\phi(3) = -x; -y$; $\phi(4) = 4(-x), 4(x)$; $\phi(\text{receiver}) = x, x, -x, -x, -x, x, x$. (d) Double-stimulated-echo experiment with bipolar gradient pulses. The phase cycle is $\phi(1) = x, x, y, y, -x, -x, -y, -y$; $\phi(2) = y, -x, -x, -y, -y, x, x, y$; $\phi(3) = \phi(7) = \phi(9) = \phi(10) = x$; $\phi(4) = -x, -x, -y, -y$; $\phi(5) = 2(-y, -y, x, x), 2(x, x, y, y)$; $\phi(6) = -x$; $\phi(8) = 16(x), 16(-x)$; $\phi(\text{receiver}) = 2(x, -x), 4(-x, x), 2(x, -x)$. Narrow and wide black rectangles represent 90° and 180° RF pulses, respectively. Rectangles with a diagonal indicate the ramped gradients. The selected coherence-transfer pathways $p(t)$ are represented for the sequences (b), (c), and (d).

constant-velocity effects (flow and convection). The coherence-transfer pathways [in vector notation (*10*)] (0, 1, 0, −1, 0, 1, 0, −1) and (0, −1, 0, 1, 0, −1, 0, −1) are selected by an appropriate phase cycle (see Fig. 1c) and, if available, orthogonal spoiler gradients during the *z*-storage periods (*6*). The velocity phase factor $B(t)$ from the first STE period is ''unwound'' during the second STE period. The first moment of the effective gradient over the whole sequence is zero. Chemical shifts are also refocused if the delay between the pulses 3 and 4 is twice that between the pulses 1 and 2 and between the pulses 5 and 6. To reduce eddy-current distortions, we use an additional longitudinal eddy-current delay T_e (*11*), which also allows both coherence-transfer pathways of opposite signs during the precession periods to be converted to observable magnetization (dashed and full lines in the coherence-transfer pathway diagrams of Fig. 1).

In order to compensate eddy-current effects, bipolar gradients have been used previously in diffusion experiments (*12*). We therefore introduce a version of the DSTE experiment with bipolar gradient pulses (Fig. 1d). The selected

coherence-transfer pathways are (0, 1, −1, 0, −1, 1, 0, 1, −1, 0, −1) and (0, −1, 1, 0, 1, −1, 0, −1, 1, 0, −1). Orthogonal spoiler gradients are also useful here to shorten the phase cycle.

Note that it is possible to merge the gradients in the center of the DSTE sequences, but due to finite gradient rise times, discrete identical gradients yield better refocusing. By using identical gradient shapes throughout the sequence, one can avoid the need for special calibration. The delays τ_1 and τ_2 in Fig. 1d need not necessarily be equal in the bipolar sequence, since chemical shifts are refocused separately in each precession period by 180° pulses.

The gradient-dependent signal attenuation,

$$f_G = \exp(-DQ_{b,c,d}), \qquad [3]$$

can be calculated (using $q = \gamma g \delta$) from Eq. [1], where

$$Q_b = q^2\left(T + \frac{2\delta}{3} + \frac{3\tau}{4}\right) \qquad [4]$$

for sequence (b),

$$Q_c = q^2\left(T + \frac{4\delta}{3} + 2\tau\right) \qquad [5]$$

for sequence (c), and

$$Q_d = q^2\left(T + \frac{4\delta}{3} + \frac{5\tau_1}{4} + \frac{\tau_2}{4}\right) \qquad [6]$$

for sequence (d). δ, τ, and T refer to the delays in Fig. 1.

The relative sensitivity of the experiments is determined by relaxation during the pulse sequences. Relaxation-dependent amplitude factors $f_R^{b,c,d}$ can be calculated from the relaxation times as

$$f_R^b = \exp\left(-2\,\frac{\delta + \tau}{T_2} - \frac{T + T_e}{T_1}\right) \qquad [7]$$

for sequence (b),

$$f_R^c = \exp\left(-4\,\frac{\delta + \tau}{T_2} - \frac{T + T_e}{T_1}\right) \qquad [8]$$

for sequence (c), and

$$f_R^d = \exp\left(-4\,\frac{\delta + (\tau_1 + \tau_2)/2}{T_2} - \frac{T + (\tau_1 - \tau_2)/2 + T_e}{T_1}\right) \qquad [9]$$

for sequence (d).

Figure 2a shows diffusion measurements on a sample of 80% glycol in DMSO-d_6 (Bruker temperature-calibration sample) at 330 K using a noncompensated sequence (Fig. 1b) and the convection-compensated sequences of Figs. 1c and 1d. The experiments were performed on a 500 MHz Bruker Avance DRX500 spectrometer using a high-resolution 5 mm TXI probe with actively shielded triple orthogonal gradients.

The diffusion constants were obtained from the gradient-dependent signal decay after phasing and integration using a monoexponential Levenberg–Marquardt fit (*13*). It can be seen that the signal from the velocity-compensated sequences exhibits a much slower decay than from the ordinary diffusion experiment and also yields the correct diffusion constant. The initial signal intensity, however, is highest in the noncompensated sequence as expected from Eqs. [7]–[9].

In our experiments, the bipolar version yields a slightly steeper decay than the monopolar sequence which, we believe, is caused by incomplete refocusing in the sequence with more pulses. This may be improved by exactly calibrating the positive and negative gradient areas especially in the high gradient range and use of composite 180° pulses. Furthermore, it is expected that the bipolar sequence performs better than the monopolar sequence on probes equipped with less effectively shielded (or unshielded) gradient coils than on the probe used here.

Figure 2b shows a plot of the measured diffusion constants of the same sample versus the reciprocal temperature. The compensated sequences show a linear behavior (on a logarithmic D scale), which corresponds to an Arrhenius-type behavior of diffusion, while the noncompensated sequence gives erratic values, e.g., a deviation by a factor of 9 at 347 K.

The examples above clearly show the power of the DSTE technique to determine diffusion constants in the presence of convection in the sample. This is particularly important for the measurements at high and low temperatures since it is very difficult to eliminate small temperature gradients even in advanced probe designs. In imaging applications, double PGSE (*14, 15*) techniques were used for velocity compensation previously, which are however unsuitable for high-resolution spectroscopy. It is also possible to reduce the effects of convection by measuring diffusion with gradients in the x, y plane. However, on many NMR probes, the z gradient is the strongest one or even the only one available. (When there are no x or y gradients available, one can easily implement extended phase cycles to remove undesired coherence-transfer pathways.) It is also expected that this method is particularly useful for diffusion measurements on macromolecules, since measurements of smaller diffusion coefficients are affected even more by convection (Eq. [1]). The advantage of the DSTE experiments applies especially to high-resolution probes used for diffusion-ordered spectroscopy (*1–6*), where long diffusion times must be used since the gradient strengths are limited. This makes the measurements

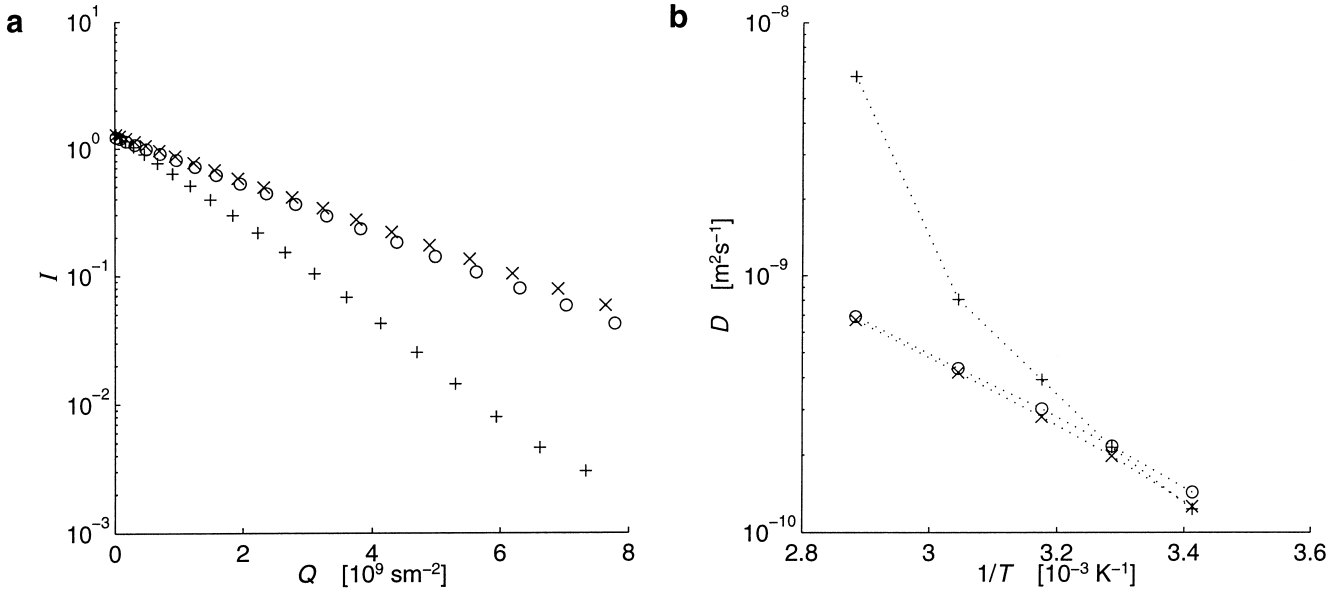

FIG. 2. (a) The signal amplitude I of the CH_2 signal of 80% glycol in DMSO-d_6 is plotted vs Q (Eqs. [3]–[6]). (+), bipolar-gradient STE sequence (Fig. 1b); (×), monopolar double STE sequence (Fig. 1c); (○), bipolar double-STE sequence (Fig. 1d). The units of I are arbitrary. Diffusion coefficients determined by fitting to the data points: $D_+ = 8.07 \times 10^{-10}$ m/s^2, $D_\times = 4.19 \times 10^{-10}$ m/s^2, $D_0 = 4.34 \times 10^{-10}$ m/s^2. (b) shows a plot of D vs $1/T$. The pulse sequence parameters were $T = 100$ ms, $\delta = 2.8$ ms, $T_e = 30$ ms, $\tau = 2$ ms, $\tau_1 = \tau_2 = 4$ ms, 90° pulse: 10.7 μs, for STE rectangular z-gradient ramps (32 increments) with $g_{max} = 63$ G/cm were used. Orthogonal sine-shaped spoiler gradients with 1 G/cm (alternating in the x and y directions) were applied for 8 ms in each z-storage period. The number of repetitions was 8 for sequences (b) and (c) and 16 for sequence (d); the relaxation delay was 4 s.

more sensitive to slow convection. The DSTE technique can also be used for compensating convection effects in the x, y plane, which is important for nonsymmetrical sample geometries.

ACKNOWLEDGMENTS

This work was supported by the ''Fonds zur Förderung der Wissenschaftlichen Forschung (FWF),'' Project P 10633-ÖCH. We are also grateful for having been able to run preliminary experiments at the MR-Centre, SINTEF UNIMED, N-7034 Trondheim, Norway.

REFERENCES

1. K. F. Morris, P. Stilbs, and C. S. Johnson, Jr., *Anal. Chem.* **66,** 211 (1995).
2. H. Barjat, G. A. Morris, S. Smart, A. G. Swanson, and S. C. R. Williams, *J. Magn. Reson. B* **108,** 170 (1995).
3. E. K. Gozansky and D. G. Gorenstein, *J. Magn. Reson. B* **111,** 94 (1996).
4. D. Wu, A. Chen, and C. S. Johnson, Jr., *J. Magn. Reson. A* **121,** 88 (1996).
5. N. Birlirakis and E. Guittet, Abstracts of the Thirteenth European Experimental NMR Conference, Paris, p. 53, May 1996.
6. A. Jerschow and N. Müller, *J. Magn. Reson. A* **123,** 222 (1996).
7. J. Lounila, K. Oikarinen, P. Ingman, and J. Jokisaari, *J. Magn. Reson. A* **118,** 50 (1996).
8. P. T. Callaghan, ''Principles of Nuclear Magnetic Resonance Microscopy,'' Oxford Univ. Press, Oxford, 1993.
9. E. J. Fordham, S. J. Gibbs, and L. D. Hall, *Magn. Reson. Imaging* **12,** 279 (1994).
10. L. Mitschang, H. Ponstingl, D. Grindrod, and H. Oschkinat, *J. Chem. Phys.* **102,** 3089 (1995).
11. D. P. Hinton and C. S. Johnson, Jr., *J. Phys. Chem.* **97,** 9064 (1993).
12. D. Wu, A. Chen, and C. S. Johnson, Jr., *J. Magn. Reson. A* **115,** 260 (1995).
13. D. W. Marquardt, *J. Soc. Ind. Appl. Math.* 431 (1963).
14. P. T. Callaghan and Y. Xia, *J. Magn. Reson.* **91,** 326 (1991).
15. Y. Xia and P. Callaghan, *Macromolecules* **24,** 4777 (1991).